



## Note

# Synthesis, crystal structure, luminescence and thermal decomposition kinetics of Eu(III) complex with 2,4-dichlorobenzoic acid and 2,2'-bipyridine

Liang Tian<sup>a,b</sup>, Ning Ren<sup>c</sup>, Jian-Jun Zhang<sup>a,\*</sup>, Hong-Mei Liu<sup>d</sup>, Ji-Hai Bai<sup>e</sup>, Hong-Mei Ye<sup>a,b</sup>, Shu-Jing Sun<sup>a,b</sup>

<sup>a</sup> Experimental Center, Hebei Normal University, Shijiazhuang, Hebei 050016, PR China

<sup>b</sup> College of Chemistry and Material Science, Hebei Normal University, Shijiazhuang 050016, PR China

<sup>c</sup> Department of Chemistry, Handan College, Handan 056005, PR China

<sup>d</sup> College of Chemistry and Pharmacy Engineering, Hebei University of Science and Technology, Shijiazhuang 050018, PR China

<sup>e</sup> Department of Compute, Hebei Normal College of Science and Technology, Qinhuangdao 066600, PR China

## ARTICLE INFO

## Article history:

Received 8 November 2008

Received in revised form 4 March 2009

Accepted 9 March 2009

Available online 16 March 2009

## Keywords:

2,4-Dichlorobenzoic acid

Europium complex

Crystal structure

Thermal analysis

Non-isothermal kinetics

Luminescence

## ABSTRACT

The complex of  $[\text{Eu}(\text{2,4-DCIBA})_3(\text{bipy})]_2$  (2,4-DCIBA = 2,4-dichlorobenzoate; bipy = 2,2'-bipyridine) was obtained and characterized by elemental analysis, IR spectra, UV spectra, luminescence spectra,  $^1\text{H}$  NMR spectra, single crystal X-ray diffraction and TG-DTG techniques. Two  $\text{Eu}^{3+}$  ions are connected by four carboxylate groups through bridging bidentate and bidentate chelating-bridging mode. The coordination number of europium ion is nine. The thermal decomposition behavior of the title complex under a static air atmosphere can be discussed by TG-DTG, SEM and IR techniques. The non-isothermal kinetics was investigated by using double equal-double steps method and Starink method. The mechanism function of the first decomposition step was determined. Meanwhile, the thermodynamic parameters ( $\Delta H^\ddagger$ ,  $\Delta G^\ddagger$  and  $\Delta S^\ddagger$ ) and kinetic parameters (activation energy  $E$  and the pre-exponential factor  $A$ ) were also calculated.

© 2009 Elsevier B.V. All rights reserved.

## 1. Introduction

Because of the various crystal structures and unique properties [1–8], the complexes of rare-earth elements with benzoic acid and some of derivatives have drawn great attention among scholars for decades. Along with in-depth studies, their application value has also attracted great attention. What deserves to be mentioned is, efficient luminescent materials may have several applications: as new rare-earth fluorescent materials, as luminescent probes in biomedical assays [9], as emitters in electroluminescent (EL) devices [10], etc. In addition, they have been used in many other fields gradually, such as pharmaceutical industries, functional material preparation. Meanwhile, thermal analysis techniques are further developed and widely used to study the thermal behavior and properties of solid materials. These studies will provide value information for understanding their potential applications.

In the previous studies [11–22], a series of ternary lanthanide complexes with benzoic acid or benzoate derivatives and nitrogen-containing ligands were prepared, and their crystal structures, thermal decomposition behaviors and non-isothermal kinetics were also reported. In this work, on the basis of the previous works, the complex  $[\text{Eu}(\text{2,4-DCIBA})_3(\text{bipy})]_2$  was synthesized. Meanwhile, the crystal structure, fluorescence spectra and thermal decomposi-

tion mechanism were studied, and the non-isothermal kinetics was discussed by using double equal-double steps method [23], and Starink method [24].

## 2. Experimental

### 2.1. Synthesis of $[\text{Eu}(\text{2,4-DCIBA})_3(\text{bipy})]_2$

$\text{EuCl}_3 \cdot 6\text{H}_2\text{O}$  (0.2 mmol), 2,4-dichlorobenzoic acid (0.6 mmol) and 2,2'-bipyridine (0.2 mmol) were dissolved, respectively, in 95%  $\text{C}_2\text{H}_5\text{OH}$  solution. The pH of 2,4-dichlorobenzoic acid solution was controlled in the range of 6–7 by addition of NaOH solution ( $1 \text{ mol L}^{-1}$ ). The two ligands were mixed and the mixture was added dropwise to the  $\text{EuCl}_3 \cdot 6\text{H}_2\text{O}$  solution, stirred continuously at room temperature for about 10 h and then deposited for 12 h. Subsequently, the precipitates were collected by filtration and then dried in desiccator. The colorless single crystals were obtained by slow evaporation of the mother solution at room temperature about a month. The Element *Anal.* Calc.: C, 42.40; H, 1.95; N, 3.19; Eu, 17.30. Found: C, 41.61; H, 1.28; N, 3.10; Eu, 16.85%.

### 2.2. Chemicals and apparatus

$\text{Eu}_2\text{O}_3$  ( $\geq 99.99\%$ ), 2,4-dichlorobenzoic acid and 2,2'-bipyridine were obtained from commercial sources and used without further purification.

\* Corresponding author. Tel.: +86 031186269386; fax: +86 031186268405.  
E-mail address: [jjzhang6@126.com](mailto:jjzhang6@126.com) (J.-J. Zhang).

The contents of carbon, hydrogen and nitrogen were acquired on a Vario-EL III element analyzer, while the metal content was assayed using EDTA titration method. Infrared spectra were recorded at room temperature from 4000 to 400  $\text{cm}^{-1}$  using a Perkin-Elmer FTIR-1730 spectrometer with the KBr discs technique. The ultraviolet spectra were recorded on a Shimadzu 2501 spectrophotometer in DMSO.  $^1\text{H}$  NMR spectra were obtained by a Bruker AVANCE500MHZ-NMR spectrometer. The single crystal X-ray diffraction data was obtained by a Bruker Apex II CCD diffractometer with graphite-monochromated Mo  $\text{K}\alpha$  radiation ( $\lambda = 0.71073 \text{ \AA}$ ) at 293 K using  $\varphi$ - $\omega$  scan technique in the range of  $1.72^\circ \leq \theta \leq 26.00^\circ$ . A semi-empirical absorption correction with the SADABS was applied. The structure was solved by direct methods using SHELXS-97 program and refined by Full-matrix least-squares on  $F^2$  using SHELXL-97 program to  $R_1 = 0.0722$   $wR_2 = 0.1751$ . The TG-DTG experiments were achieved using a Perkin-Elmer TGA7 thermogravimetric analyzer. The heating rate was 3, 5, 7, 10, 15  $^\circ\text{C min}^{-1}$  from ambient to 950  $^\circ\text{C}$  under a static air atmosphere. The fluorescence spectra were measured on an F-4500 Hitachi spectrophotometer in the solid state at room temperature. Small amount of the sample was dispersed regularly on the sample holder and Au was sprayed for 15 min with Hitachi IB-5. Then they were observed by the Hitachi S-570 scanning electron microscope.

### 3. Results and discussion

#### 3.1. Ultraviolet spectra

The UV spectra data of the ligands and its complex were depicted with DMSO solution as reference. The complex and ligands have the strong  $\pi \rightarrow \pi^*$  transition absorption. The UV absorption spectra of the complex show maximum absorption peak at 280 nm, while the band for the 2,4-DCIBA ligand is about 260 nm. This phenomenon can be explained by the expansion  $\pi$ -conjugated system that caused by the metal coordination [25]. In addition, the maximum absorption band of bipy at 280 nm is similar to that in the complex, but it is noteworthy that the molar extinction coefficient in the same wavelength is greatly enhanced (from 0.28 to 0.38), suggesting that it has formed bigger conjugated system, namely forming chelating ring.

#### 3.2. Infrared spectra

The characteristic bands of the ligands and its complex are displayed in Table 1. The IR spectrum of the complex shows the characteristic absorption of the carboxylate group at 1614  $\text{cm}^{-1}$  for asymmetric stretching and at 1411  $\text{cm}^{-1}$  for symmetric stretching ( $\Delta = 203 \text{ cm}^{-1}$ ). While the characteristic band of carboxylate group at 1699  $\text{cm}^{-1}$  attributed to the free ligand 2,4-DCIBA disappears completely. The results clearly show the oxygen atoms in carboxylate groups participate in coordination to  $\text{Eu}^{3+}$  ion [26]. The separation ( $\Delta$ ) of the complex similar to corresponding sodium salt ( $\Delta = 193 \text{ cm}^{-1}$ ) is considered indicative of bidentate bridging carboxylate groups [27]. Furthermore, the appearance of the band of  $\nu(\text{Eu}-\text{O})$  at 419  $\text{cm}^{-1}$  also indicates the conclusions above. Meanwhile, the bands of  $\nu_{\text{CN}}(1578 \text{ cm}^{-1})$  and  $\delta_{\text{CH}}(992 \text{ cm}^{-1}, 757 \text{ cm}^{-1})$  of a bipy ligand shift to higher wave numbers around at 1588, 1014 and 761  $\text{cm}^{-1}$  in the spectra of the complex, indicating

that the coordination of nitrogen atoms of a bipy ligand to  $\text{Eu}^{3+}$  ion [28].

#### 3.3. $^1\text{H}$ NMR spectra

$^1\text{H}$  NMR spectra of the ligands and its complex were obtained at room temperature in deuterated solvent (DMSO). The chemical shift of  $^1\text{H}$  NMR spectra of the complex and ligands are displayed in Table 2. The spectral line of the proton (COOH) of free 2,4-DCIBA ligand in  $^1\text{H}$  NMR spectra disappears on complexation. The facts indicate that the oxygen atoms of the carboxyl group are coordinated to  $\text{Eu}^{3+}$  ion [29]. Meanwhile, chemical shift  $\delta_{\text{H}}$  of benzol ring moves to high magnetic field in  $^1\text{H}$  NMR spectra after coordination. Because the carboxyl group directly bonded with  $\text{Eu}^{3+}$  while coordinating instead of H atom. As a result, electron cloud moved to benzol ring, making electron density equilibration, which leads to the moving of the shift  $\delta_{\text{H}}$  at benzol ring to high magnetic field.

The chemical shifts of bipy do not change after coordination. It may be caused by steric effect of bipy. The new Eu-N bonds are formed via the non-hybridized p orbit of bipy nitrogens share lone electron pairs with  $\text{Eu}^{3+}$ . But as the crystal structure of the title complex shown, 2,4-dichlorobenzoic acids are around to bipy. And so, there will have large steric hindrance to the two bulky pyridine rings. As a result of it, the bond lengths of the new formed Eu-N bonds get longer. Because of the weak coordination between  $\text{Eu}^{3+}$  and bipy nitrogen, the electro cloud density of bipy system is nearly not affected, and this fact results in the unchanged chemical shift.

#### 3.4. Luminescent properties

The luminescence spectrum excited at 396 nm was recorded at room temperature as shown in Fig. 1. The sample gives rise to red light emission under UV excitation. The emission spectrum for the title complex is composed of the characteristic emission peaks of Eu (III) arising from  $^5\text{D}_0 \rightarrow ^7\text{F}_0$  (579 nm),  $^5\text{D}_0 \rightarrow ^7\text{F}_1$  (592 nm) and  $^5\text{D}_0 \rightarrow ^7\text{F}_2$  (615 nm), respectively. The luminescence intensity of  $^5\text{D}_0 \rightarrow ^7\text{F}_2$  transition emission is strongly dependent on the chemical environments of  $\text{Eu}^{3+}$ . And Fig. 1 shows the intensity of  $^5\text{D}_0 \rightarrow ^7\text{F}_2$  electric dipole transition is much greater than that of  $^5\text{D}_0 \rightarrow ^7\text{F}_1$  magnetic dipole transition, indicating that there is no inversion symmetry at the site of  $\text{Eu}^{3+}$  ion [30].

#### 3.5. Crystal structure determination

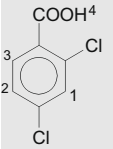
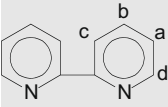
The crystal structure of the title complex is displayed in Fig. 2. Crystallographic data for the title complex are presented in Table 3 and the selected bond lengths and angles listed in Table 4.

Each  $\text{Eu}^{3+}$  is nine coordinated to two nitrogen atoms from one 2,2'-bipyridine molecule, two oxygen atoms from one bidentate chelating carboxylate group, two oxygen atoms from two bidentate bridging carboxylate groups, and three oxygen atoms from two bidentate chelating-bridging carboxylate groups. The coordination polyhedron around  $\text{Eu}^{3+}$  shown in Fig. 3 is a capped square antiprism geometry, and the capping donor atom is O3. The molecules are interlinked by super-molecular network structure along the [1,0,1] direction via  $\pi$ - $\pi$  stacking interaction as shown in Fig. 4.

**Table 1**  
IR absorption for the ligands and complex ( $\text{cm}^{-1}$ ).

Compounds	$\nu_{\text{CN}}$	$\delta_{\text{CH}}$	$\nu_{\text{CO}}$	$\nu_{\text{as}}(\text{COO}^-)$	$\nu_{\text{s}}(\text{COO}^-)$	$\nu(\text{RE}-\text{O})$
Bipy	1578	992	757			
2,4-HDCIBA			1699			
$[\text{Eu}(2,4\text{-DCIBA})_3(\text{bipy})_2]$	1588	1014	751	1614	1411	419

**Table 2**  
<sup>1</sup>HNMR data for the ligands and complex.

Compounds	$\delta$ (ppm)							
	$\delta_1$	$\delta_2$	$\delta_3$	$\delta_4$	$\delta_a$	$\delta_b$	$\delta_c$	$\delta_d$
	7.88	7.71	7.57	13.53				
					7.45	7.95	8.40	8.69
[Eu(2,4-DCIBA) <sub>3</sub> (bipy)] <sub>2</sub>	7.06	6.96	6.53		7.46	7.96	8.40	8.70

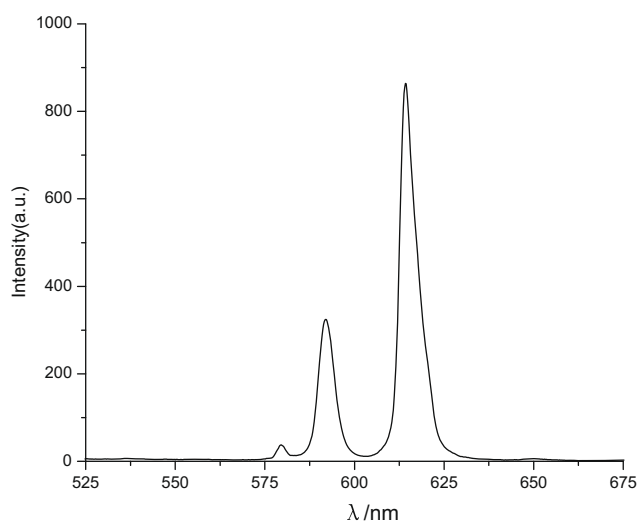


Fig. 1. Luminescence spectra of complex [Eu(2,4-DCIBA)<sub>3</sub>(bipy)]<sub>2</sub>.

In the title complex, the length of Eu–O bond is in the range of 2.353(7)–2.632(8) Å, and the mean bond length is 2.444 Å. While the length of Eu–N bond between 2.552(9) Å and 2.581(8) Å with an average length of 2.567 Å is longer than the Eu–O bond, indicating that Eu–O bond is stronger than Eu–N bond, which is in accordance with the results of thermal decomposition process. In the binuclear molecule, the Eu–O bond distance of bidentate bridging carboxyl groups are smaller than those of the chelating carboxyl groups. The reason is probably due to the stronger strain in the four-membered ring of chelating coordination [31].

### 3.6. Thermal decomposition of the complex

The TG–DTG curves of [Eu(2,4-DCIBA)<sub>3</sub>(bipy)]<sub>2</sub> with a heating rate of 10 °C min<sup>-1</sup> are shown in Fig. 5. The data of thermal decomposition are listed in Table 5. The SEM pictures of the complex [Eu(2,4-DCIBA)<sub>3</sub>(bipy)]<sub>2</sub> at RT, 289.68 °C and 871.99 °C are given in Fig. 6a–c.

As is shown from the DTG curve, the thermal decomposition process of the title complex can be divided into two stages. The first stage occurs from 137.84 °C to 289.68 °C with the mass loss of 17.38% (the theoretical mass loss is 17.79%), which is equivalent to the loss of 2bipy. The IR spectra of the residue at 289.68 °C shows that the absorption band of C=N at 1588 cm<sup>-1</sup> disappears. Compared with Fig. 6a and b, the appearance of the title complex

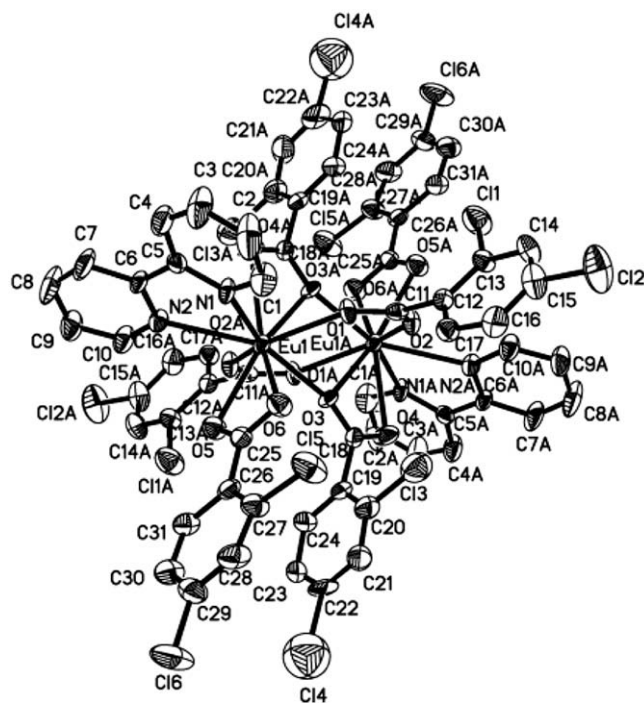
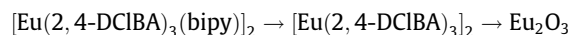


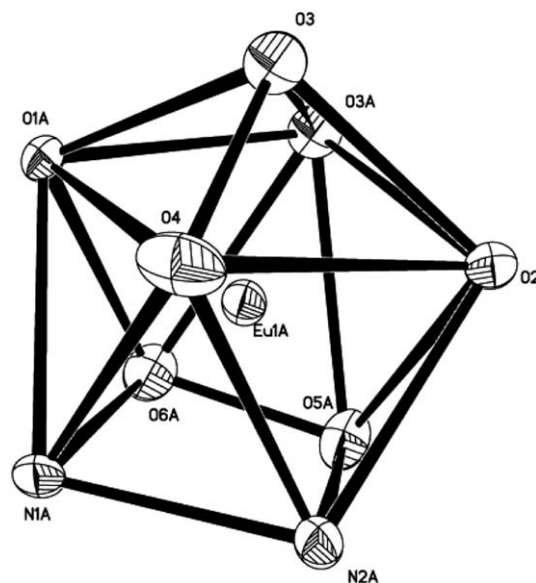
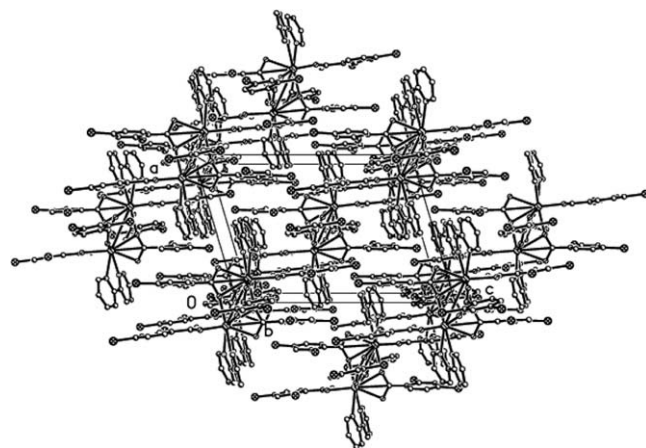
Fig. 2. Molecular Structure of the title complex.

changed from smooth-surface to a cracked crystal. The second stage occurs at 289.68–871.99 °C with the mass loss of 62.06% (the theoretical mass loss is 62.18%) and corresponds to the loss of C<sub>42</sub>H<sub>18</sub>Cl<sub>12</sub>O<sub>9</sub>. As shown in the IR spectra of the residue, the bands of the asymmetric vibrations  $\nu_{as}(\text{COO}^-)$  at 1614 cm<sup>-1</sup> and symmetric vibrations  $\nu_s(\text{COO}^-)$  at 1411 cm<sup>-1</sup> disappear. It can be seen that the cracked crystal broke up into even smaller granules from the Fig. 6c. The characteristic absorption band of the residue as shown in the IR spectra is similar to the standard sample spectrum of Eu<sub>2</sub>O<sub>3</sub>. Therefore, the final product at 871.99 °C is Eu<sub>2</sub>O<sub>3</sub>. The total weight loss of the thermal decomposition process of the title complex is 79.44% (the theoretical mass loss is 79.97%). Based on the analysis above, the thermal decomposition process of [Eu(2,4-DCIBA)<sub>3</sub>(bipy)]<sub>2</sub> can be denoted in the following scheme:



**Table 3**  
Crystal data and structure refinement for [Eu(2,4-DCIBA)<sub>3</sub>(bipy)]<sub>2</sub>.

Item	Data
Empirical formula	C <sub>62</sub> H <sub>46</sub> Cl <sub>12</sub> Eu <sub>2</sub> N <sub>4</sub> O <sub>12</sub>
Formula weight	1756.25
Temperature (K)	293(2)
Wavelength (Å)	0.71073
Crystal system, space group	monoclinic, P2(1)/n
Unit cell dimensions	
<i>a</i> (Å)	11.94674(19)
<i>b</i> (Å)	17.2743(3)
<i>c</i> (Å)	16.955(3)
$\alpha$ (°)	90
$\beta$ (°)	106.600(3)
$\gamma$ (°)	90
<i>V</i> (Å <sup>3</sup> )	3353.2(10)
<i>Z</i> , calculated density (Mg/m <sup>3</sup> )	2, 1.739
Absorption coefficient (mm <sup>-1</sup> )	2.394
<i>F</i> (000)	1720
Crystal size (mm)	0.390 × 0.252 × 0.189
$\theta$ range for data collection (°)	1.72–26.00
Limiting indices	−14 ≤ <i>h</i> ≤ 12, −18 ≤ <i>k</i> ≤ 21, −20 ≤ <i>l</i> ≤ 16
Reflections collected/unique [ <i>R</i> <sub>int</sub> ]	17636/6581 [0.1641]
Completeness to $\theta = 26.00$	99.9%
Absorption correction	empirical
Maximum and minimum transmission	1.0000 and 0.8338
Refinement method	full-matrix least-squares on <i>F</i> <sup>2</sup>
Data/restraints/parameters	6581/6/410
Goodness-of-fit (GOF) on <i>F</i> <sup>2</sup>	0.944
Final <i>R</i> indices [ <i>I</i> > 2 $\sigma$ ( <i>I</i> )]	<i>R</i> <sub>1</sub> = 0.07224, <i>wR</i> <sub>2</sub> = 0.1751
<i>R</i> indices (all data)	<i>R</i> <sub>1</sub> = 0.1234, <i>wR</i> <sub>2</sub> = 0.1937
Largest difference peak and hole (e Å <sup>-3</sup> )	2.741 and −1.425

**Fig. 3.** Coordination geometry of Eu<sup>3+</sup> ion.**Fig. 4.** Crystal packing diagram of the title complex.**Table 4**  
Bond lengths (Å) and angles (°) for [Eu(2,4-DCIBA)<sub>3</sub>(bipy)]<sub>2</sub>.

Eu(1)#1–O(3)	2.632(8)	Eu(1)#1–O(5)#1	2.424(8)
Eu(1)#1–O(4)	2.517(8)	Eu(1)#1–O(6)#1	2.428(8)
Eu(1)#1–N(1)#1	2.552(9)	Eu(1)#1–O(1)#1	2.388(7)
Eu(1)#1–N(2)#1	2.581(8)	Eu(1)#1–O(3)#1	2.364(6)
Eu(1)#1–O(2)	2.353(7)	O(2)–Eu(1)#1–N(1)#	137.2(3)
O(2)–Eu(1)#1–O(3)#	74.8(2)	O(3)#–Eu(1)#1–N(1)#	148.0(3)
O(2)–Eu(1)#1–O(1)#	135.0(3)	O(1)#–Eu(1)#1–N(1)#	79.1(3)
O(3)#–Eu(1)#1–O(1)#	75.2(2)	O(5)#–Eu(1)#1–N(1)#	96.6(3)
O(2)–Eu(1)#1–O(5)#	80.7(3)	O(6)#–Eu(1)#1–N(1)#	74.6(3)
O(3)#–Eu(1)#1–O(5)#	85.0(3)	O(3)#–Eu(1)#1–N(2)#	146.6(3)
O(1)#–Eu(1)#1–O(5)#	126.8(3)	O(1)#–Eu(1)#1–N(2)#	138.1(3)
O(2)–Eu(1)#1–O(6)#	129.6(3)	O(5)#–Eu(1)#1–N(2)#	74.1(3)
O(3)#–Eu(1)#1–O(6)#	81.1(3)	O(3)#–Eu(1)#1–O(3)	72.9(2)
O(1)#–Eu(1)#1–O(6)#	76.8(3)	O(1)#–Eu(1)#1–O(3)	70.3(2)
O(5)#–Eu(1)#1–O(6)#	53.3(3)	O(5)#–Eu(1)#1–O(3)	146.2(3)
O(2)–Eu(1)#1–O(4)	87.0(3)	O(6)#–Eu(1)#1–O(3)	142.1(3)
O(3)#–Eu(1)#1–O(4)	122.5(3)	O(4)–Eu(1)#1–O(3)	49.8(2)
O(1)#–Eu(1)#1–O(4)	81.7(3)	O(2)–Eu(1)#1–C(18)	77.4(3)
O(5)#–Eu(1)#1–O(4)	145.7(3)	O(3)#–Eu(1)#1–C(18)	98.1(3)
O(6)#–Eu(1)#1–O(4)	142.4(3)	O(5)#–Eu(1)#1–C(18)	156.2(3)

#1 −*x* + 2, −*y* + 2, −*z* + 2.

### 3.7. Kinetics of the first decomposition stage

The activation energy *E* of the first decomposition stage has been calculated by Starink method [24]. The equation is as follows:

$$\ln \frac{\beta}{T_f^{1.92}} = -1.0008 \frac{E}{RT_f} + C \quad (1)$$

By substituting *T<sub>f</sub>* and  $\beta$  obtained from the experiment into Eq. (1), *E* is determined from the slope of plots of  $\ln(\beta/T_f^{1.92})$  versus  $1/T_f$ .

Fig. 7 shows the relationship between *E* and  $\alpha$ . The values of activation energy *E* change slightly with  $\alpha$ , suggesting the first decomposition stage is a single step reaction [32]. Therefore, the

*E*, *A* and probable mechanism function can be determined by means of double equal-double steps method [23]. The Ozawa iteration equation [33] is as follows:

$$\ln \frac{\beta}{H(x)} = \left\{ \ln \left[ \frac{0.0048AE}{R} \right] - \ln G(\alpha) \right\} - 1.0516 \frac{E}{RT} \quad (2)$$

$$H(x) = \frac{\exp(-x)}{0.0048 \exp(-1.0516x)} h(x)$$

$$h(x) = \frac{x^4 + 18x^3 + 86x^2 + 96x}{x^4 + 20x^3 + 120x^2 + 240x + 120}$$

$$\ln G(\alpha) = \ln \left( \frac{0.0048AEH(x)}{R} \right) - 1.0516 \frac{E}{RT} - \ln \beta = a + b \ln \beta \quad (3)$$

where *G*( $\alpha$ ) is the integral mechanism function, *T* the absolute temperature, *A* the pre-exponential factor, *R* the gas constant, *E* the apparent activation energy and  $\beta$  the linear heating rate.

By substituting the values of  $\alpha$ ,  $\beta$  in Table 6 and various conversion functions [34] into Eq. (3), using the linear least-squares method with  $\ln G(\alpha)$  versus  $\ln \beta$ , the linear correlation coefficient

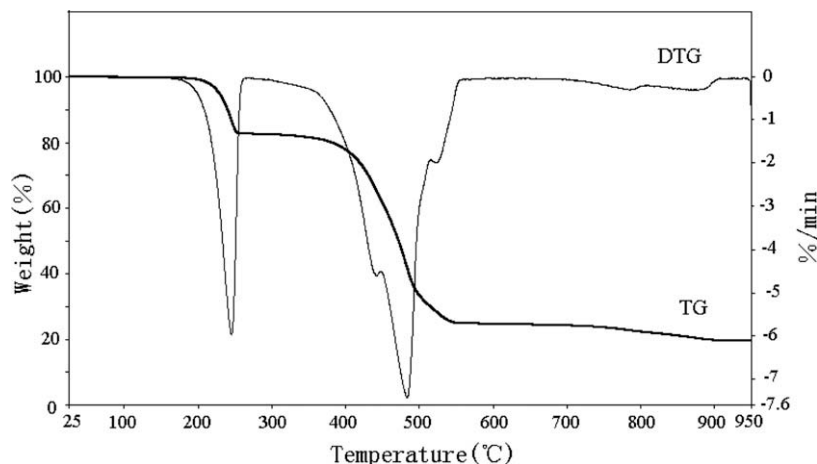


Fig. 5. TG–DTG curves of the title complex at a heating rate of  $10\text{ }^{\circ}\text{C min}^{-1}$ .

**Table 5**  
Thermal decomposition data for  $[\text{Eu}(\text{2,4-DCIBA})_3(\text{bipy})_2]$  ( $\beta = 10\text{ }^{\circ}\text{C min}^{-1}$ ).

Stage	Temperature range ( $^{\circ}\text{C}$ )	DTG peak temperature ( $^{\circ}\text{C}$ )	Mass loss (%)		Probable composition of removed groups	Intermediate
			TG	Theory		
I	137.84–289.68	245.11	17.38	17.79	2bipy	$[\text{Eu}(\text{2,4-DCIBA})_3]_2$
II	289.68–871.99	483.32	62.06	62.18	$\text{C}_{42}\text{H}_{18}\text{Cl}_{12}\text{O}_9$	$\text{Eu}_2\text{O}_3$

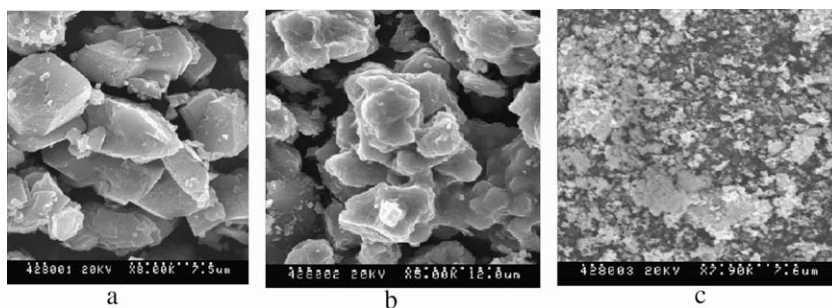


Fig. 6. SEM pictures of the  $[\text{Eu}(\text{2,4-DCIBA})_3(\text{bipy})_2]$  at (a) RT; (b)  $289.68\text{ }^{\circ}\text{C}$  and (c)  $871.99\text{ }^{\circ}\text{C}$ .

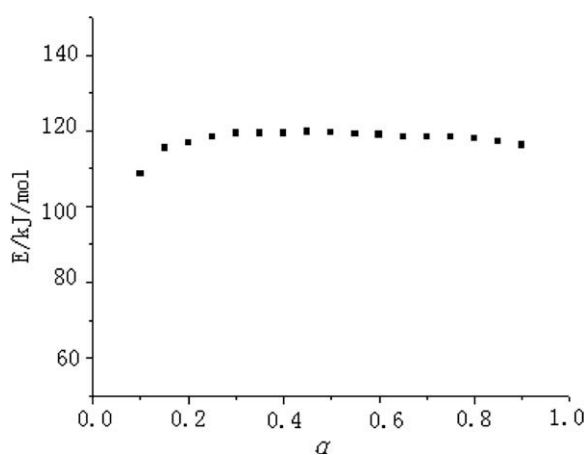


Fig. 7. The relationship of  $E$  and  $\alpha$  of the first decomposition stage for the title complex.

$r$ , the slope  $b$  and the intercept  $a$  at the different temperatures were obtained. The integrant results are listed in Table 7.

As seen from Table 7, it can be concluded that only the coefficients  $r$  of the function no. 25 is best while the slope  $b$  is close to  $-1$ . So the probable mechanism function of the title complex is  $G(\alpha) = \alpha$ ,  $f(\alpha) = 1$ . Therefore, it can be decided that the reaction mechanism in the first stage is the boundary reaction. The kinetic equation is  $\frac{d\alpha}{dt} = \frac{A}{\beta} \exp(-\frac{E}{RT})$ .

The activation energy is inaccurate by plots of  $\ln\beta$  versus  $1/T$  based on the traditional isoconversional method, as it neglects the variation of  $H(x)$  against  $x$ . However, iterative calculations considering the change can give the exact value of activation energy by means of plots of  $\ln(\beta/H)$  versus  $1/T$ , no matter how little or how great the  $E/RT$  value of the reaction is. The value of activation energy is iteratively calculated by Ozawa iteration method [33] according to Eq. (2), until the absolute difference of  $(E_i - E_{i-1})$  is less than a defined small quantity such as  $0.1\text{ kJ mol}^{-1}$ .

By substituting the values of  $\alpha$ ,  $\beta$  and  $T$  in Table 8 and the corresponding mechanism function determined above into Eq. (2), via the linear least-squares method with  $\ln\beta/H(x)$  versus  $1/T$ . The activation energy  $E$  can be calculated from the value of the slope and the pre-exponential factor  $A$  can also be calculated from the value of the intercept. The results are listed in Table 9.

The thermodynamic parameters of activation can be calculated from the equations [35,36]:

**Table 6**Conversion degrees measured for given the same temperatures on the TG–DTG curves of [Eu(2,4-DCIBA)<sub>3</sub>(bipy)]<sub>2</sub> at different heating rates: (Stage I).

T (K)	$\alpha$				
	$\beta = 3\text{ }^{\circ}\text{C min}^{-1}$	$\beta = 5\text{ }^{\circ}\text{C min}^{-1}$	$\beta = 7\text{ }^{\circ}\text{C min}^{-1}$	$\beta = 10\text{ }^{\circ}\text{C min}^{-1}$	$\beta = 15\text{ }^{\circ}\text{C min}^{-1}$
483.61	0.2878	0.1585	0.1000	0.0770	0.0534
489.81	0.4335	0.2456	0.1500	0.1192	0.0813
494.27	0.5726	0.3358	0.2000	0.1629	0.1098
497.66	0.7014	0.4183	0.2500	0.2034	0.1385
500.47	0.8196	0.5021	0.3000	0.2466	0.1641
502.87	0.9072	0.5849	0.3500	0.2883	0.1943
504.96	0.9603	0.6648	0.4000	0.3294	0.2193

**Table 7**Integrant of the results from the linear least-squares method at different temperatures for [Eu(2,4-DCIBA)<sub>3</sub>(bipy)]<sub>2</sub>: (Stage I).

T (K)	Function no.	a	b	r
483.61	15	0.2811	-0.8495	-0.9924
	25	-0.6473	-1.0491	-0.9943
	35	0.2648	-0.8306	-0.9976
489.81	15	0.2112	-0.8864	-0.9904
	25	0.1136	-1.0431	-0.9934
	35	0.3037	-0.7141	-0.9956
494.27	15	0.3588	-0.9268	-0.9881
	25	0.2329	-1.0309	-0.9925
	35	0.2925	-0.6011	-0.9897
497.66	15	0.4888	-0.9745	-0.9859
	25	0.3150	-1.0149	-0.9926
	35	0.2615	-0.5004	-0.9825
500.47	14	0.5581	-0.9294	-0.9838
	25	0.3829	-1.0045	-0.9931
	35	0.2306	-0.4194	-0.9683
502.87	9	1.5713	-3.4176	-0.9724
	25	0.4157	-0.9677	-0.9928
	35	0.1943	-0.3422	-0.9547
504.96	6	0.8097	-2.6356	-0.9872
	25	0.4350	-0.9313	-0.9924
	35	0.1676	-0.2868	-0.9361

$$A \exp(-E/RT) = \nu \exp(-\Delta G^{\ddagger}/RT) \quad (4)$$

$$\Delta H^{\ddagger} = E - RT \quad (5)$$

$$\Delta G^{\ddagger} = \Delta H^{\ddagger} - T\Delta S^{\ddagger} \quad (6)$$

where  $\nu$  is the Einstein Vibration frequency,  $\Delta G^{\ddagger}$  is the Gibbs free enthalpy of activation,  $\Delta H^{\ddagger}$  is the enthalpy of activation,  $\Delta S^{\ddagger}$  is entropy of activation. The values of entropy, enthalpy and the Gibbs free energy of activation at the peak temperature acquired on the basis of Eqs. (4)–(6) are shown in Table 10. As seen in Table 10,

**Table 8**

The values of temperatures at the same degree of conversion for the different heating rate on TG curves for the title complex (Stage I).

$\alpha$	T (K)				
	$\beta = 3\text{ }^{\circ}\text{C min}^{-1}$	$\beta = 5\text{ }^{\circ}\text{C min}^{-1}$	$\beta = 7\text{ }^{\circ}\text{C min}^{-1}$	$\beta = 10\text{ }^{\circ}\text{C min}^{-1}$	$\beta = 15\text{ }^{\circ}\text{C min}^{-1}$
0.10	466.57	478.01	483.61	487.33	492.85
0.15	473.51	482.88	489.81	493.24	498.94
0.20	477.91	486.98	494.27	497.35	503.42
0.25	481.42	490.08	497.66	500.58	506.94
0.30	484.25	492.66	500.47	503.47	509.78
0.35	486.57	494.91	502.87	505.88	512.33
0.40	488.52	496.98	504.96	507.97	514.48
0.45	490.40	498.70	506.97	509.86	516.36
0.50	492.04	500.36	508.78	511.59	518.23
0.55	493.48	501.82	510.38	513.14	519.82
0.60	495.02	503.23	511.90	514.81	521.59
0.65	496.28	504.60	513.19	516.16	523.27
0.70	497.59	505.84	514.57	517.62	524.64
0.75	498.81	507.14	515.87	518.83	526.03
0.80	500.02	508.26	517.23	520.21	527.44
0.85	501.34	509.45	518.64	521.46	529.08
0.90	502.59	510.88	520.04	523.05	530.74

**Table 9**The values of the kinetic parameters computed by use of the plot of  $\ln \beta/H(x)$  vs.  $1/T$ .

$\alpha$	E (kJ mol <sup>-1</sup> )	A × 10 <sup>14</sup> (min <sup>-1</sup> )	r
0.10	109.03	2.49	-0.9846
0.15	115.89	14.91	-0.9909
0.20	117.24	21.39	-0.9906
0.25	118.94	33.25	-0.9911
0.30	119.77	41.33	-0.9913
0.35	119.83	42.20	-0.9915
0.40	119.94	43.73	-0.9914
0.45	120.37	48.83	-0.9906
0.50	120.08	45.50	-0.9902
0.55	119.75	42.06	-0.9900
0.60	119.59	40.27	-0.9905
0.65	118.87	33.75	-0.9915
0.70	118.91	33.94	-0.9914
0.75	118.98	34.34	-0.9913
0.80	118.50	30.31	-0.9916
0.85	117.71	24.61	-0.9909
0.90	116.75	19.07	-0.9914
	118.13(average)	32.47(average)	

**Table 10**

The thermodynamic parameters of the title complex.

$\beta$ (°C min <sup>-1</sup> )	$\Delta H^{\ddagger}$ (kJ mol <sup>-1</sup> )	$\Delta G^{\ddagger}$ (kJ mol <sup>-1</sup> )	$\Delta S^{\ddagger}$ (J mol <sup>-1</sup> K <sup>-1</sup> )	T <sub>p</sub> (K)
3	113.91	94.23	39.45	500.46
5	113.89	93.86	39.29	509.89
7	113.83	93.56	39.17	517.50
10	113.81	93.45	39.13	520.12
15	113.76	93.24	39.04	525.68
	113.84 <sup>a</sup>	93.67 <sup>a</sup>	39.22 <sup>a</sup>	

<sup>a</sup> An average value.

the values of  $\Delta G^\ddagger$  are more than 0, indicating that the decomposition reaction for the title complex is not spontaneous reaction.

#### 4. Conclusions

The complex was synthesized by the reaction of  $\text{EuCl}_3 \cdot 6\text{H}_2\text{O}$ , 2,4-dichlorobenzoic acid and 2,2'-bipyridine. The crystal structure of the  $[\text{Eu}(\text{2,4-DCIBA})_3(\text{bipy})_2]$  shows that the carboxylic groups coordinated to  $\text{Eu}^{3+}$  with bridging bidentate, bidentate chelating and bidentate chelating-bridging modes. The coordination number is nine. The mechanism function of the first step for the title complex is  $G(\alpha) = \alpha$ ,  $f(\alpha) = 1$ . The activation energy  $E$ , the pre-exponential factor  $A$ , the enthalpy of activation  $\Delta H^\ddagger$ , the Gibbs free energy of activation  $\Delta G^\ddagger$  and the entropy of activation  $\Delta S^\ddagger$  are  $118.13 \text{ kJ mol}^{-1}$ ,  $32.47 \times 10^{14} \text{ min}^{-1}$ ,  $113.84 \text{ kJ mol}^{-1}$ ,  $93.67 \text{ kJ mol}^{-1}$  and  $39.22 \text{ J mol}^{-1} \text{ K}^{-1}$ , respectively.

#### Acknowledgements

This project was supported by the National Natural Science Foundation of China (No. 20773034), the Natural Science Foundation of Hebei Province (No. B2007000237) and Science Foundation of Hebei Normal University (No. L2006Z06).

#### Appendix A. Supplementary material

CCDC 686510 contains the supplementary crystallographic data for this paper. These data can be obtained free of charge from The Cambridge Crystallographic Data Centre via [www.ccdc.cam.ac.uk/data\\_request/cif](http://www.ccdc.cam.ac.uk/data_request/cif). Supplementary data associated with this article can be found, in the online version, at [doi:10.1016/j.ica.2009.03.010](https://doi.org/10.1016/j.ica.2009.03.010).

#### References

- [1] L.P. Jin, S.X. Lu, S.Z. Lu, *Polyhedron* 15 (1996) 4069.
- [2] X. Li, L.P. Jin, Y.H. Wang, S.Z. Lu, J.H. Zhang, *Chinese J. Chem.* 20 (2002) 352.
- [3] Y. Li, F.K. Zheng, X. Liu, W.Q. Zou, G.C. Guo, C. Z. Lu, J.S. Huang, *Inorg. Chem.* 45 (2006) 6308.
- [4] X. Li, Z.Y. Zhang, H.B. Song, *J. Mol. Struct.* 751 (2005) 33.
- [5] X. Li, Z.Y. Zhang, Y.Q. Zou, *Eur. J. Inorg. Chem.* 14 (2005) 2909.
- [6] Y.H. Wan, L.P. Zhang, L.P. Jin, S. Gao, S.Z. Lu, *Inorg. Chem.* 42 (2003) 4985.
- [7] G.Q. Li, Y. Li, W.Q. Zou, Q.Y. Chen, F.K. Zheng, G.C. Guo, *Chinese J. Struct. Chem.* 26 (2007) 575.
- [8] S. Y. Niu, J. Jin, X.L. Jin, Z.Z. Yang, *Solid State Sci.* 4 (2002) 1103.
- [9] S. Pandya, J.H. Yu, D. Parker, *Dalton Trans.* (2006) 2757.
- [10] H. Xin, F.Y. Li, M. Shi, Z.Q. Bian, C.H. Huang, *J. Am. Chem. Soc.* 125 (2003) 7166.
- [11] L. Tian, N. Ren, J.J. Zhang, S.J. Sun, H.M. Ye, J.H. Bai, R.F. Wang, *J. Chem. Eng. Data* 54 (2009) 69.
- [12] J.J. Zhang, X.L. Xu, N. Ren, H.Y. Zhang, L. Tian, *Int. J. Chem. Kinet.* 40 (2008) 66.
- [13] H.Y. Zhang, K.Z. Wu, J.J. Zhang, S.L. Xu, N. Ren, J.H. Bai, L. Tian, *Synthetic Met.* 158 (2008) 157.
- [14] X.L. Xu, J.J. Zhang, H.F. Yang, N. Ren, H.Y. Zhang, *J. Chem. Sci.* 62b (2007) 51.
- [15] H.Y. Zhang, J.J. Zhang, N. Ren, S.L. Xu, Y.H. Zhang, L. Tian, H.H. Song, *J. Alloy. Compd.* 466 (2008) 281.
- [16] X.L. Xu, J.J. Zhang, N. Ren, H.Y. Zhang, *Russ. J. Coord. Chem.* 33 (8) (2007) 622.
- [17] J.J. Zhang, N. Ren, J.H. Bai, S.L. Xu, *Int. J. Chem. Kinet.* 39 (2007) 67.
- [18] N. Ren, J.J. Zhang, Y.H. Guo, M.Q. Sun, S.L. Xu, H.Y. Zhang, *Chem. Res. Chinese U.* 23 (2007) 489.
- [19] J.J. Zhang, N. Ren, S.L. Xu, *Chinese J. Chem.* 25 (2007) 125.
- [20] H.Y. Zhang, J.J. Zhang, N. Ren, J.H. Bai, S.P. Wang, R.F. Wang, *Int. J. Chem. Kinet.* 40 (2008) 607.
- [21] H.Y. Zhang, J.J. Zhang, N. Ren, S.L. Xu, J.H. Bai, L. Tian, *J. Alloy. Compd.* 464 (2008) 277.
- [22] L.J. Xu, S.P. Wang, R.F. Wang, J.J. Zhang, *J. Coord. Chem.* 61 (2008) 237.
- [23] J.J. Zhang, N. Ren, *Chinese J. Chem.* 22 (2004) 1459.
- [24] M.J. Starink, *Thermochim. Acta* 404 (2003) 163.
- [25] B.L. An, M.L. Gong, M.X. Li, J.M. Zhang, *J. Mol. Struct.* 687 (2004) 1.
- [26] Y.Z. Shi, X.Z. Sun, Y.H. Jiang, *Spectra and Chemical Identification of Organic Compounds*, Science and Technology Press, Nan Jing, 1988. p. 98.
- [27] G.B. Deacon, R.J. Phillips, *Coord. Chem. Rev.* 33 (1980) 227.
- [28] R.F. Wang, L.P. Jin, M.Z. Wang, S.H. Huang, X.T. Chen, *Acta Chim. Sinica* 53 (1995) 39.
- [29] J.J. Zhang, R.F. Wang, Y.P. Gao, *Chinese J. Spectrosc. Lab.* 13 (1996) 4.
- [30] R.H. Zhang, P.W. Shen, *Rare Earth Element Chemistry*, Tianjin Science and Technology Press, Tianjin, 1987. p. 70.
- [31] X. Li, L.P. Jin, Y.H. Wan, *Chinese J. Chem.* 20 (2002) 352.
- [32] Z.R. Lu, Y. C Ding, Y. Xu, B.L. Li, Y. Zhang, *J. Inorg. Chem. (in Chinese)* 21 (2005) 181.
- [33] Z. Gao, M. Nakada, I. Amasski, *Thermochim. Acta* 369 (2001) 137.
- [34] R.Z. Hu, S.L. Gao, F.Q. Zhao, Q.Z. Shi, T.L. Zhang, J.J. Zhang, *Thermal Analysis Kinetics*, 2nd ed., Science Press, Beijing, 2008. p. 151.
- [35] J. Straszko, M. Olstak-Humienik, J. Mozejko, *Thermochim. Acta* 292 (1997) 145.
- [36] M. Olstak-Humienik, J. Mozejko, *Thermochim. Acta* 344 (2000) 73.